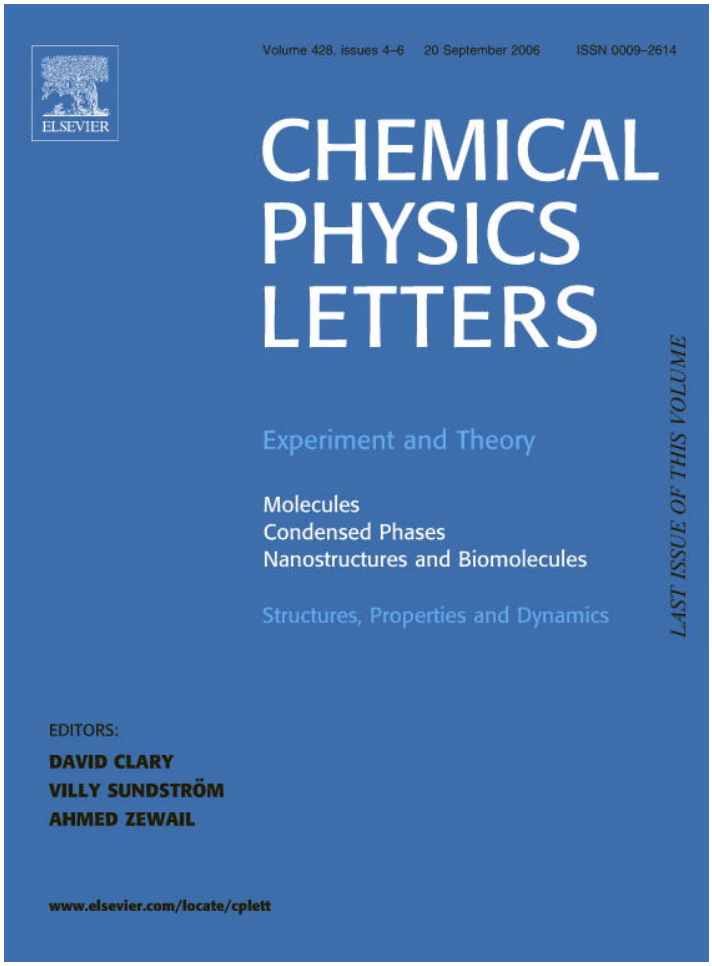

Available online at www.sciencedirect.com
ScienceDirect
Chemical Physics Letters 428 (2006) 343–347
CHEMICAL PHYSICS LETTERS
www.elsevier.com/locate/cplett

# Sonochemical synthesis of ferromagnetic core–shell $Fe_3O_4$–FeP nanoparticles and FeP nanoshells

C.G. Hu [a,b], Y. Li [c], J.P. Liu [c], Y.Y. Zhang [d], G. Bao [d], B. Buchine [a], Z.L. Wang [a,*]

[a] School of Materials Science and Engineering, Georgia Institute of Technology, Atlanta, GA 30332-0245, USA
[b] Department of Applied Physics, Chongqing University, Chongqing 400044, China
[c] Department of Physics, University of Texas at Arlington, Arlington, TX 76019, USA
[d] Department of Biomedical Engineering, Georgia Institute of Technology and Emory University, Atlanta, GA 30332-0245, USA

Received 7 May 2006; in final form 2 July 2006
Available online 22 July 2006

**Abstract**

Polycrystalline iron phosphide coated iron oxide and hollow iron phosphide nanoparticles were synthesized by sonichemistry. Structure analysis indicated that the diameters of these nanoparticles were less than 14 nm, and the core–shell and hollow nanoparticles are $Fe_3O_4$–FeP and FeP, respectively. Magnetic measurement demonstrated that both the core–shell $Fe_3O_4$–FeP and hollow FeP nanoparticles exhibited ferromagnetic behaviors.




## 1. Introduction

As compared to bulk materials, nanoscale materials exhibit large surface areas and size-dependent electronic, optical, magnetic, chemical, and thermal properties. Magnetic nanoparticles have been widely studied due to their potential applications in biomedical fields such as biomolecule separation [1–3], targeted drug delivery [4,5], cancer diagnosis and treatment [6], DNA separation/detection and sequencing of oligonucleotides [7,8], and magnetic resonance imaging [9]. On the other hand, surface modification of nanoparticles with different inorganic shells (core–shell nanostructures) has become an important strategy to functionalize nanomaterials. Such modification has generated some very interesting physical and chemical properties of the nanostructured materials that have shown important technological applications. For example, the $SiO_2$ coated $Fe_2O_3$–CdSe quantum dots (QDs) nanocomposite particles preserved the unique magnetic property of $\gamma$-$Fe_2O_3$ as well as the optical property of CdSe QDs [10]. Bimagnetic core–shell FePt–$Fe_3O_4$ nanoparticles can be transformed into hard magnetic nanocomposite with enhanced energy products upon reductive annealing [11]. Procedures leading to novel inorganic core–shell structures with controlled dimensions on both core and shell and new functionality have also been reported [12–14].

The studies on nanostructures of metal phosphides were much immature in comparison to other semiconductor materials because of difficulties in synthetic chemistry [15]. Many of the bulk metal phosphide materials are technically important as phosphorescent, magnetic, and electronic materials [16–18]. They are important in the study of magnetism because the interatomic spacing and the anion electronegativity lie in an intermediate range between those for metals and for the oxides [18]. Traditionally, bulk iron phosphides have been prepared by a variety of high-temperature methods [17,19,20] and sonochemical methods [21]. Ultrafine powder of iron phosphides was also synthesized by a solvothermal method [22], but the morphology was ill-defined and the average particle size was too large (~200 nm in diameter). Over the past few years, the preparation of nanostructured metal phosphides has gained significant interest due to the need to explore the size-dependent physical properties of these materials. Nanoparticles and nanowires of $Fe_2P$, FeP and other metal

* Corresponding author. Fax: +1 404 894 9140.
*E-mail address:* zhong.wang@mse.gatech.edu (Z.L. Wang).

0009-2614/$ - see front matter © 2006 Elsevier B.V. All rights reserved.
doi:10.1016/j.cplett.2006.07.037

phosphides have been prepared recently [23–26]. However, to the best of our knowledge, nanocomposite iron phosphide coated iron oxide and hollow iron phosphide nanoparticles have not been reported.

Here, we report synthesis and characterization of $Fe_3O_4$–FeP core–shell nanoparticles with $Fe_3O_4$ core of 5–10 nm and FeP shell of 2–3 nm, and FeP hollow nanoparticles with outer-diameter of 5–10 nm and inner-diameter of 3–8 nm. Both $Fe_3O_4$–FeP core–shell and FeP hollow nanoparticles exhibit ferromagnetic behaviors.

## 2. Experiments

We have used a novel one-step sonochemical route to prepare core–shell iron phosphide-iron oxide and hollow iron phosphide nanoparticles. Briefly, trioctylphosphine (TOP) is used to react with iron pentacarbonyl and acts as P source for the formation of iron phosphide, while trioctylphosphine oxide (TOPO) is used to control size and growth morphology of resulting materials. In a typical experiment, 5 g of TOPO (99+% from Sigma) and 6 mL of TOP (90% from Sigma) were mixed (TOPO in TOP of 50 wt%) and then sonicated until the TOPO totally dissolved in the TOP. Next, 0.5 mL of stock solution 1 (1 mL of $Fe(CO)_5$ (99.99% from Sigma) dissolved in 4 mL of TOP) was quickly injected into the dissolved TOPO/TOP mixture under aerobic condition while it was continuously sonicated in a sealed bottle. The temperature was around 65–70 °C in water bath. At each 30 min interval, a 0.2 mL portion of liquid was extracted from the reaction solution to monitor the growth process, and 0.2 mL of stock solution 1 was injected to keep the total volume unchanged. The removed liquid was dispersed in hexane and centrifuged at 14000 rpm for 60 min. The sediment from centrifuged sample was washed several times with ethanol or acetone, and redispersed in hexane.

The dimension of core–shell and hollow structured nanoparticles was characterized using transmission electron microscopy (TEM). Samples for TEM analysis were prepared by drying a hexane dispersion of the particles on amorphous carbon coated copper grids. Philips X-ray diffractometer and energy-dispersive X-ray spectroscopy (EDS) were used to investigate the chemical composition of the as-synthesized samples. Particles were imaged using TEM JEOL 100CX II and SEM LEO 1530 (T-FE). The structure detail of the core–shell and hollow nanoparticles was characterized using HRTEM Hitachi HF-2000 (FEG). Magnetic studies were carried out using a MPMS2 Quantum Design SQUID magnetometer with fields up to 7 T and temperatures from 5 to 300 K.



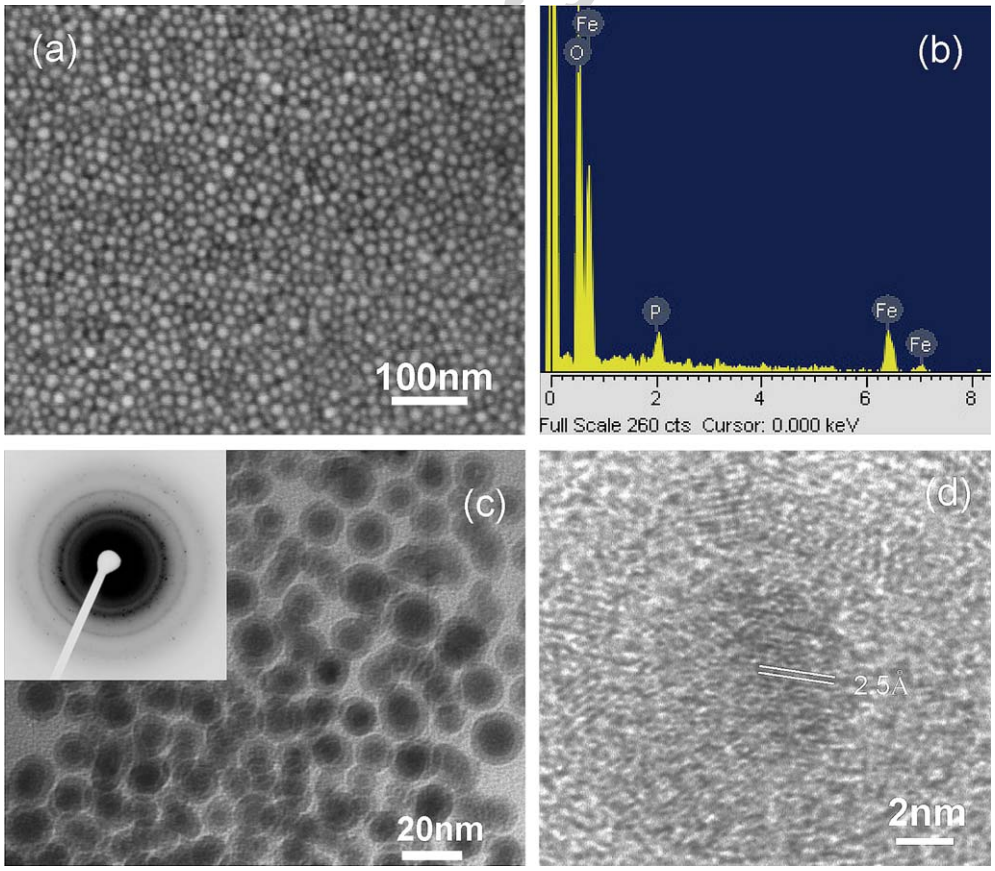


Fig. 1. Characterization of core–shell $Fe_3O_4$–FeP particles, which have been sonochemically synthesized for 4 h: (a) SEM image, (b) EDS, (c) TEM image and (d) HRTEM image of core–shell $Fe_3O_4$–FeP particles with spacing of 2.5 Å, corresponding to plane ⟨3 1 1⟩ of $Fe_3O_4$. The inset in (c) is diffraction pattern of core–shell $Fe_3O_4$–FeP particles. It shows the polycrystalline particles.

## 3. Results and discussion

We found that the reaction time did not affect the morphology of synthesized particles, but there were more hollow particles than core–shell particles at the first 1 h. A large amount of core–shell particles could be produced after 3 h. core–shell particles were obtained by centrifuge the redispersed sample in hexane at 14000 rpm for 30 min and then picking the sediment in the bottom. Fig. 1 is the characterization of core–shell particles, which have been sonochemically synthesized for 4 h. SEM image shows the shape of particles and the size is about 8–13 nm with core 5–10 nm and shell 2–3 nm Fig. 1a. EDS analysis exhibits the average atomic ratio of Fe:O:P is around 4:4.2:1 Fig. 1b. TEM image gives the details of the core–shell structure of the particles, and the diffraction pattern of the core–shell particles in the inset displays crystal structure Fig. 1c. HRTEM image further tell us that both the core and the shell are polycrystalline Fig. 1d, and the labeled spacing of 2.5 Å corresponds to plane distance of $Fe_3O_4$ ⟨3 1 1⟩.

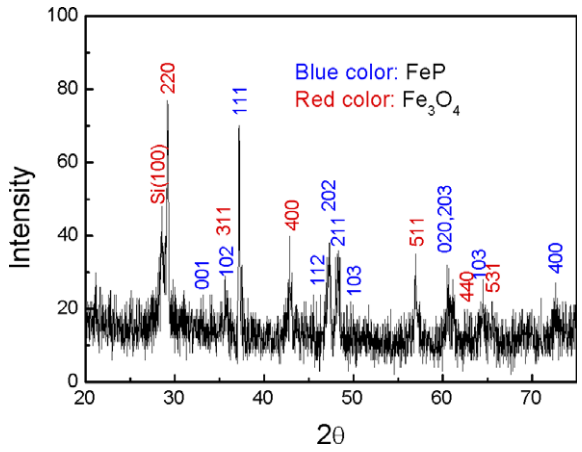


Fig. 2. XRD pattern of the core–shell $Fe_3O_4$–FeP particles synthesized for 4 h. The blue and red labels are for FeP (JCPDS 78-1443) and $Fe_3O_4$ (JCPDS 89-3854) respectively. (For interpretation of the references to color in this figure legend, the reader is referred to the web version of this article.)

In order to demonstrate identity of the particles, we carried out X-ray diffraction experiment. All blue peaks in the XRD pattern in Fig. 2 can be indexed to the orthorhombic cell of the FeP phase with space group Pnma(62), lattice constant $a = 5.193(1)$ Å, $b = 3.099(1)$ Å, and $c = 5.792(1)$ Å (JCPDS 78-1443). The red peaks in the XRD can be indexed to cubic cell of the $Fe_3O_4$ phase with space group $Fd\bar{3}m$ (2 2 7), lattice constant $a = 8.394$ Å (JCPDS 89-3854). Based on HRTEM images and hollow FeP particles' XRD analysis in Fig. 4, we can distinguish the core is $Fe_3O_4$ and the shell is FeP.

The hollow particles were obtained simply by extracting the upper part of the solution after centrifuging the redispersed sample in hexane at 14000 rpm for 30 min. Fig. 3 is the characterization of hollow particles, which have been sonochemically synthesized for 4 h. TEM image shows that the hollow particles have outer-diameters of 5–10 nm and inner-diameters of 3–8 nm and several core–shell particles still remain Fig. 3a. HRTEM image and diffraction pattern exhibit the polycrystalline hollow structure Fig. 3b with spacings of 3.9 Å and 2.4 Å, corresponding to planes of ⟨0 0 2⟩ and ⟨1 1 1⟩ of FeP, respectively. The XRD pattern in Fig. 4 further demonstrates the orthorhombic cell of the FeP phase with space group Pnma, lattice constant $a = 5.193(1)$ Å, $b = 3.099(1)$ Å, and $c = 5.792(1)$ Å (JCPDS

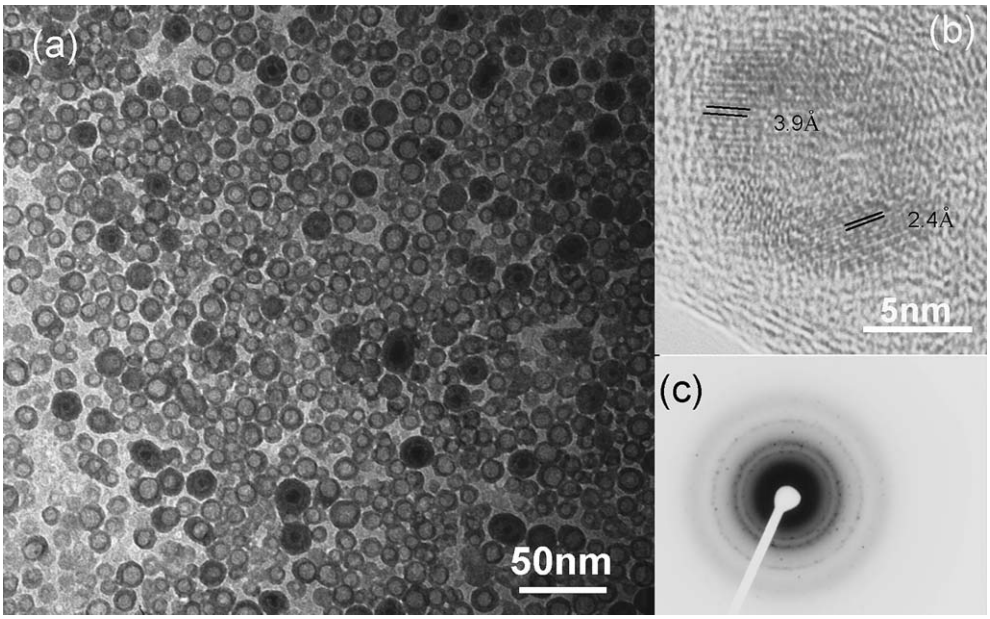


Fig. 3. Characterization of hollow FeP particles, which have been sonochemically synthesized for 4 h. (a) TEM image, (b) HRTEM image and (c) diffraction pattern of hollow FeP particles showing the polycrystalline particles with spacings of 3.9 Å and 2.4 Å, corresponding to planes of ⟨0 0 2⟩ and ⟨1 1 1⟩ of FeP, respectively.

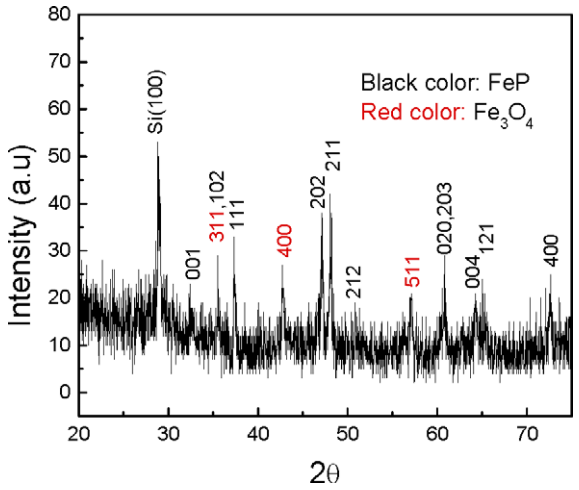


Fig. 4. XRD pattern of hollow FeP particles synthesized for 4 h. The black labels are for FeP (JCPDS 78-1443). As there are still a small amount of $Fe_3O_4$–FeP core–shell particles mixed in the sample, the blue labels show the existence of $Fe_3O_4$ (JCPDS 89-3854). (For interpretation of the references to color in this figure legend, the reader is referred to the web version of this article.)

78-1443), which gives another identification of shell FeP phase in core–shell particles. As there are still some core–shell $Fe_3O_4$–FeP particles mixed in the sample, the XRD pattern has weak peaks of $Fe_3O_4$ in it.

Sonichemistry is a very special method for nanomaterial synthesis. The chemical effects of ultrasound do not come from a direct interaction with molecular species. Instead, sonochemistry and sonoluminescence arise from acoustic cavitation: the formation, growth, and implosive collapse of bubbles in a liquid. Cavitational collapse produces intense local heating (~5000 K), high pressures (~1000 atm), and enormous heating and cooling rates (> $10^9$ K/s). Acoustic cavitation provides a unique interaction of energy and matter, and ultrasonic irradiation of liquids causes high energy chemical reactions to occur, often accompanied by the emission of light. [27,28]. To understand the formation mechanism of these hollow and core–shell particles, we have performed an experiment without TOPO. The results are amorphous powder. TOPO is usually used as a capping reagent to promote selective anisotropic growth of nanocrystals [29]. The fact that hollow or core–shell particles cannot be obtained without TOPO, indicates it plays a key role in the formation process. Additionally, TOPO could promote atomic exchange between nanoparticles, a requirement for size distribution focusing and kinetic control [11,30]. The TOPO in the mixture not only functions as a cosolvent but also as phosphor source [11]. We assume that the intermediate species could decompose to produce FeP by breaking the Fe–C and P–C bonds under local high

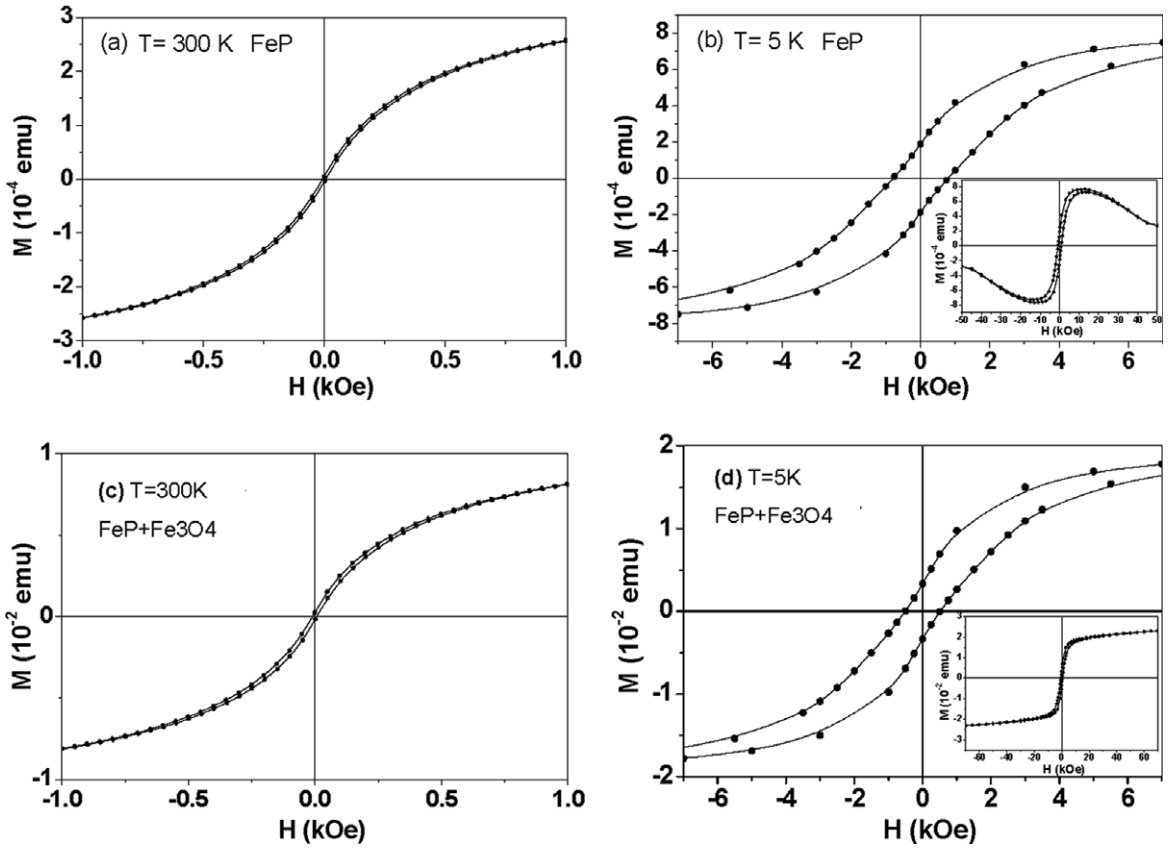


Fig. 5. Magnetic behavior for hollow FeP particles synthesized for 4 h. The *M–H* loop at room (a) and low temperature (b) the inset shows the whole *M–H* loop from −7 to 7 T at 5 K temperature. Magnetic behavior for core–shell $Fe_3O_4$–FeP particles synthesized for 4 h. The *M–H* loop at room temperature (c) and low temperature (d) The inset shows the whole *M–H* loop from −7 to 7 T at 5 K temperature.

temperature after the stock solution is injected and it grows into hollow particle due to the strong vibration as well as capping effect of TOPO. Some decomposed $Fe(CO)_5$ reacts with residual oxygen to form $Fe_3O_4$ inside the shell, and produces core–shell $Fe_3O_4$–FeP particles.

Magnetic properties of the hollow FeP and core–shell $Fe_3O_4$–FeP particles have been studied using AGM (Alternating Gradient Magnetometer) and SQUID (Superconducting Quantum Interference Devices) at room temperature and low temperature under magnetic field up to 7 T. Fig. 5a–b shows the $M$–$H$ loop at room temperature and low temperature for the hollow FeP particles. The inset in Fig. 5b shows the whole $M$–$H$ loop from −7 to 7 T at 5 K. As shown in Fig. 5a, hollow FeP exhibits soft ferromagnetic behavior. There is a very tiny hysteresis effect at room temperature. The coercivity is only 7 Oe. Under low temperature ($T = 5$ K), the magnetic behavior becomes significant; the coercivity Hc is about 760 Oe (Fig. 5b). Due to very small sample, the diamagnetic signal appears under high field. The decreasing of $M$–$H$ curve at high field arises from contribution of organic glue. Fig. 5c–d gives the $M$–$H$ loop at room temperature and low temperature for the core–shell $Fe_3O_4$–FeP particles under magnetic field up to 7 T. The inset in Fig. 5d shows the whole $M$–$H$ loop from −7 to 7 T at 5 K. For the core–shell sample, due to the magnetic contribution of $Fe_3O_4$ and a little bit bigger sample size, there is no significant diamagnetic behavior. The $M$–$H$ curve shows a soft ferromagnetic behavior. There is almost no hysteresis behavior at room temperature. The low temperature measurement shows that the coercivity reaches 500 Oe, which is smaller than that of sample FeP. Because $Fe_3O_4$ is magnetically a much soft material, at 10 K with coercivity ranging from 200 Oe for 4 nm to 450 Oe for 16 nm nanoparticles [11], the increasing of softer phase such as $Fe_3O_4$ results in a decreasing of coercivity.

## 4. Conclusion

Polycrystalline core–shell $Fe_3O_4$–FeP and hollow FeP particles have been synthesized in the TOPO/TOP solvent systems via a simple one-step sonochemical route. The size of the core–shell particles synthesized for 4 h are in the range of 8–13 nm with the core of 5–10 nm and the shell of 2–3 nm, and shelled-particles are 5–10 nm. The magnetic experiments show soft ferromagnetic behaviors for both the core–shell $Fe_3O_4$–FeP particles and FeP shelled-particles. And they exhibit almost no hysteresis behavior at room temperature; but under low temperature ($T = 5$ K), the magnetic behavior becomes significant. The coercivity Hc is about 760 Oe for hollow FeP particles and 500 Oe for core–shell $Fe_3O_4$–FeP particles.

## Acknowledgements

This work is funded by NSFC (No. 60376032, 90406024), NSF, DARPA and NASA, and NIH (1U01HL80711-01). We thank J. Zhou for HRTEM examinations.

## References

[1] C. Wilhelm, F. Gazeau, J.C. Bacri, Eur. Biophys. J. 31 (2002) 118.
[2] J.M. Perez, F.J. Simeone, Y. Saeki, L. Josephson, R. Weissleder, J. Am. Chem. Soc. 125 (2003) 10192.
[3] J.D. Fan, J.G. Lu, R.S. Xu, R. Jiang, Y. Gao, J. Colloid Interf. Sci. 266 (2003) 215.
[4] N. Nakamura, J.G. Burgess, K. Yagiuda, S. Kudo, T. Sakaguchi, T. Matsunaga, Anal. Chem. 65 (1993) 2030.
[5] P.K. Gupta, C.T. Hung, F.C. Lam, D.G. Perrier, Int. J. Pharm. 43 (1988) 167.
[6] A. Jordan et al., J. Magn. Magn. Mater. 225 (2001) 118.
[7] P.S. Doyle, J. Bibette, A. Bancaud, J.L. Viovy, Science 295 (2002) 2237.
[8] L. Josephson, J.M. Perez, R. Weissleder, Angew. Chem., Int. Ed. 40 (2001) 3204.
[9] Z. Li, H. Chen, B. Bao, M.Y. Gao, Chem. Mater. 16 (2004) 1391.
[10] D.K. Yi, S.T. Selvan, S.S. Lee, G.C. Papaefthymiou, D. Kundaliya, J.Y. Ying, J. Am. Chem. Soc. 127 (2005) 4990.
[11] H. Zeng, J. Li, Z.L. Wang, J.P. Liu, S. Sun, Nano Letters 4 (2004) 187.
[12] E.E. Carpenter, S. Calvin, R.M. Stroud, V.G. Harris, Chem. Mater. 15 (2003) 3245.
[13] N.S. Sobal, U. Ebel, H. Mohwald, M. Giersig, J. Phys. Chem. B 107 (2003) 7351.
[14] V. Skumryev, S. Stoyanov, Y. Zhang, G. Hadjipanayis, D. Givord, J. Nogues, Nature 423 (2003) 850.
[15] J.R. Heath, J.J. Shiang, Chem. Soc. Rev. 27 (1998) 65.
[16] B. Arinsson, T. Landstrom, S. Rundquist, Borides, Silicides and Phosphides, Wiley, New York, 1965.
[17] N.N. Greenwood, A. Earnshaw, Chemistry of the Elements, Pergamon Press, New York, 1994, p. 563.
[18] B.F. Stein, R.H. Walmsley, Phys. Rev. B 148 (1966) 933.
[19] D.E.C. Corbridge, Phosphorus: An Outline of its Chemistry, Biochemistry and Technology, fifth edn., Elsevier, New York, 1995.
[20] J.C. Fitzmaurice, A.L. Hector, I.P. Parkin, J. Mater. Sci. Lett. 13 (1994) 1.
[21] J.D. Sweet, D.J. Casadonte, Ultrason. Sonochem. 8 (2001) 97.
[22] Y.L. Gu, F. Guo, Y.T. Qian, H.G. Zheng, Z.P. Yang, Mater. Res. Bull. 37 (2002) 1101.
[23] K.L. Stamm, J.C. Gamo, G.Y. Liu, S.L. Brock, J. Am. Chem. Soc. 125 (2003) 4038.
[24] C.M. Lukehart, S.B. Milne, S.R. Stock, R.D. Shull, J.E. Wittig, Nanotechnology 622 (1996) 195.
[25] C. Qian, F. Kim, L. Ma, F. Tsui, P.D. Yang, J. Liu, J. Am. Chem. Soc. 126 (2004) 1195.
[26] J. Park et al., Angew. Chem., Int. Ed. 43 (2004) 2282.
[27] K.S. Suslick, fourth edn.Kirk-Othmer Encyclopedia of Chemical Technology, vol. 26, J. Wiley & Sons, New York, 1998, p. 517.
[28] K.S. Suslick et al., Phil. Trans. Roy. Soc. London A 357 (1999) 335.
[29] J. Cheon, N.J. Kang, S.M. Lee, J.H. Lee, J.H. Yoon, S.J. Oh, Am. Chem. Soc. 126 (2004) 1590.
[30] V.F. Puntes, K.M. Krishnan, A.P. Alivisatos, Science 291 (2001) 2115.